

# A new crustal model as input for the European strength map

*M. Tesauro*<sup>(1,2)</sup>, *M. Kaban*<sup>(2)</sup>, *S. Cloetingh*<sup>(1)</sup>

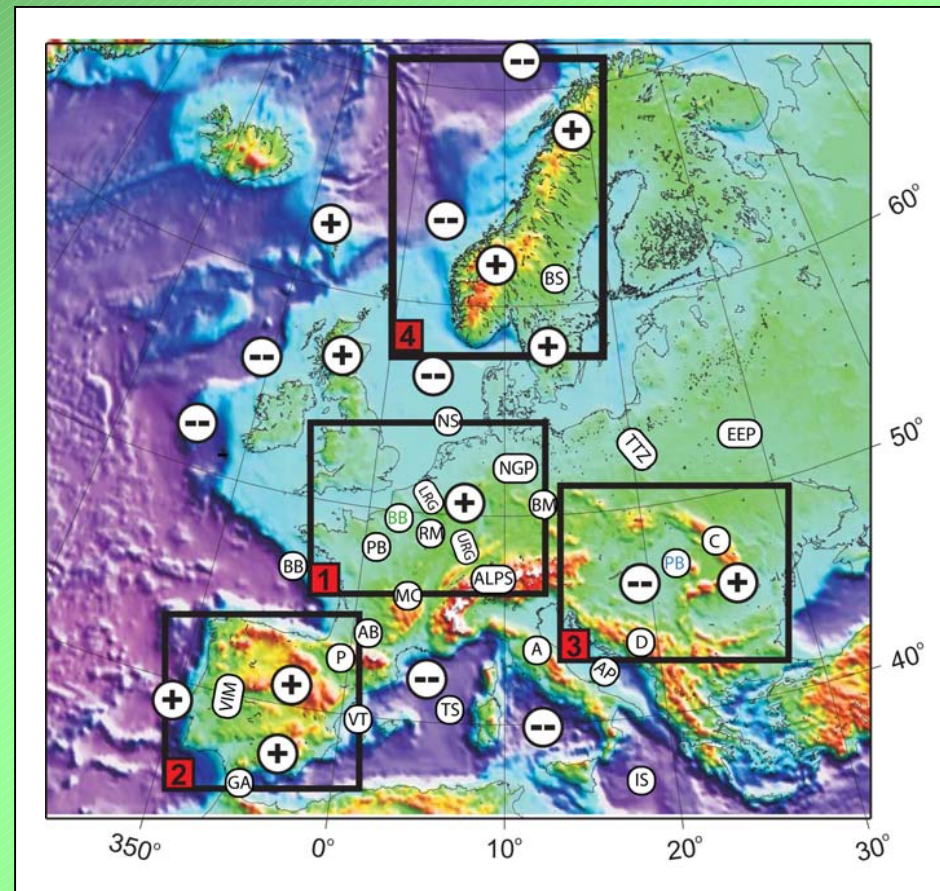
(1) Netherlands Research Centre for Integrated Solid Earth science,  
Faculty of Earth and Life Science, Vrije Universiteit

(2) GeoForschungsZentrum (GFZ)



# Europe: the area of study

- (1) Northwestern European platform
- (2) Microcontinent Iberia
- (3) Carpathian–Pannonian Basin
- (4) North Atlantic Margin



EEP = East European Platform, BS = Baltic Shield, TTZ = Tesseyre–Tornquist zone, C=Carpathians, PB=Pannonian Basin, NGP=North German Plane, BM=Bohemian Massif, D=Dinarides, NS=North Sea, LRG=Lower Rhine Graben, URG=Upper Rhine Graben, RM=Rhenish Massif, BRB=Brabant Massif, PB=Paris Basin, MC=Massif Central, BB=Bay of Biscay, AB=Aquitaine Basin, P=Pyrenees, VIM=Varican Iberian Platform, VT=Valencia Trough, TS=Tyrrhenian Sea, GA=Gibraltar Arc, AP=Adriatic Plate, A=Apennines, IS=Ionian Sea



# Perspectives

## New crustal model

- Sedimentary Thickness
- Main crystalline crust discontinuities
- *P*-Wave average velocity within the layers

## Data of the mantle structure

- Seismic tomography
- mineral physics
- geothermal data

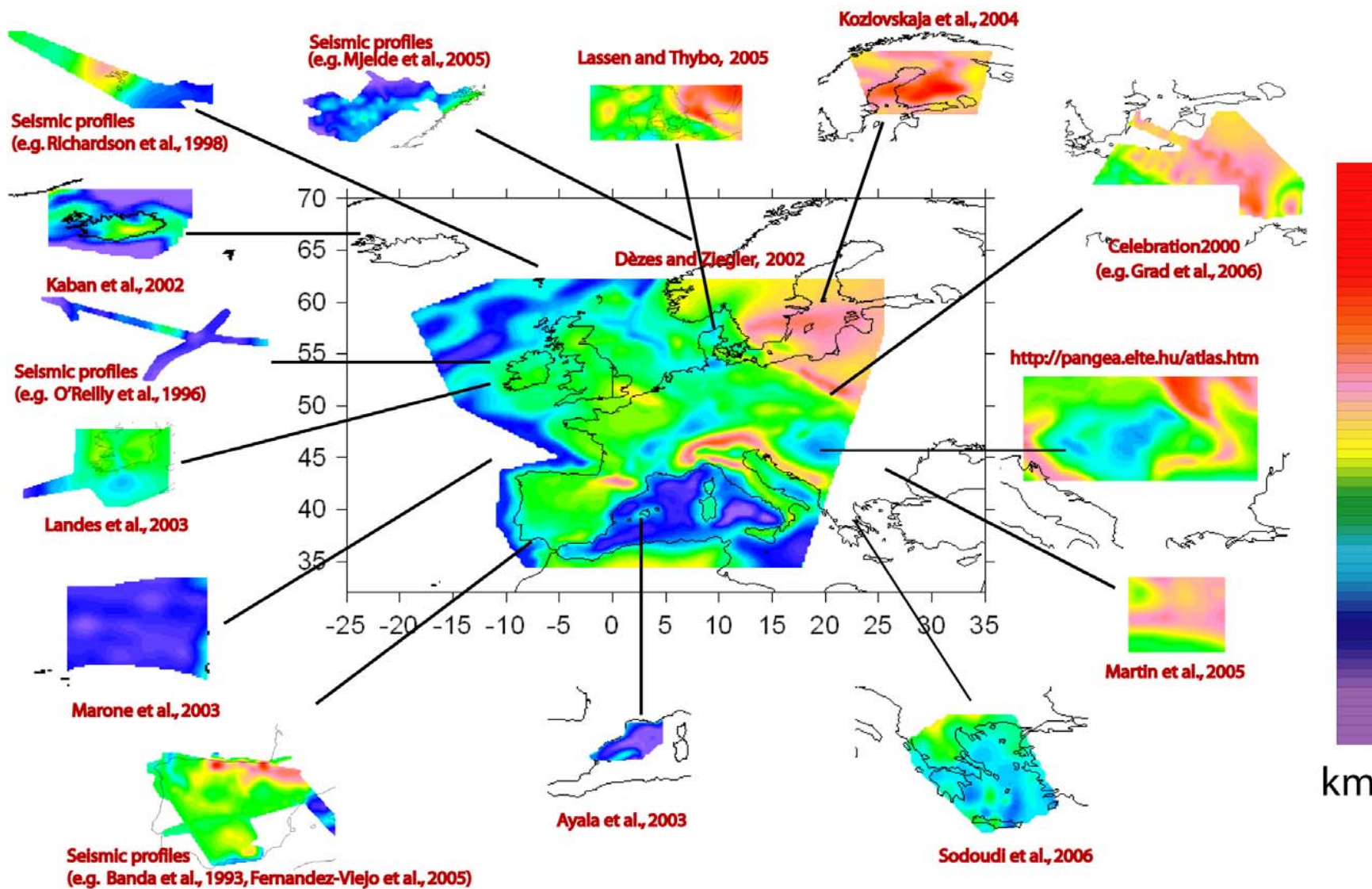


- Recalculation of temperature distribution in the lithosphere (using outdated heat flow map and tomography data)
- Construction of a new gravity model of the lithosphere
- Improvements of the 3D strength model (including lateral variation of physical parameters)
- Prediction of the 3D spatial distribution of the current stress and strain field

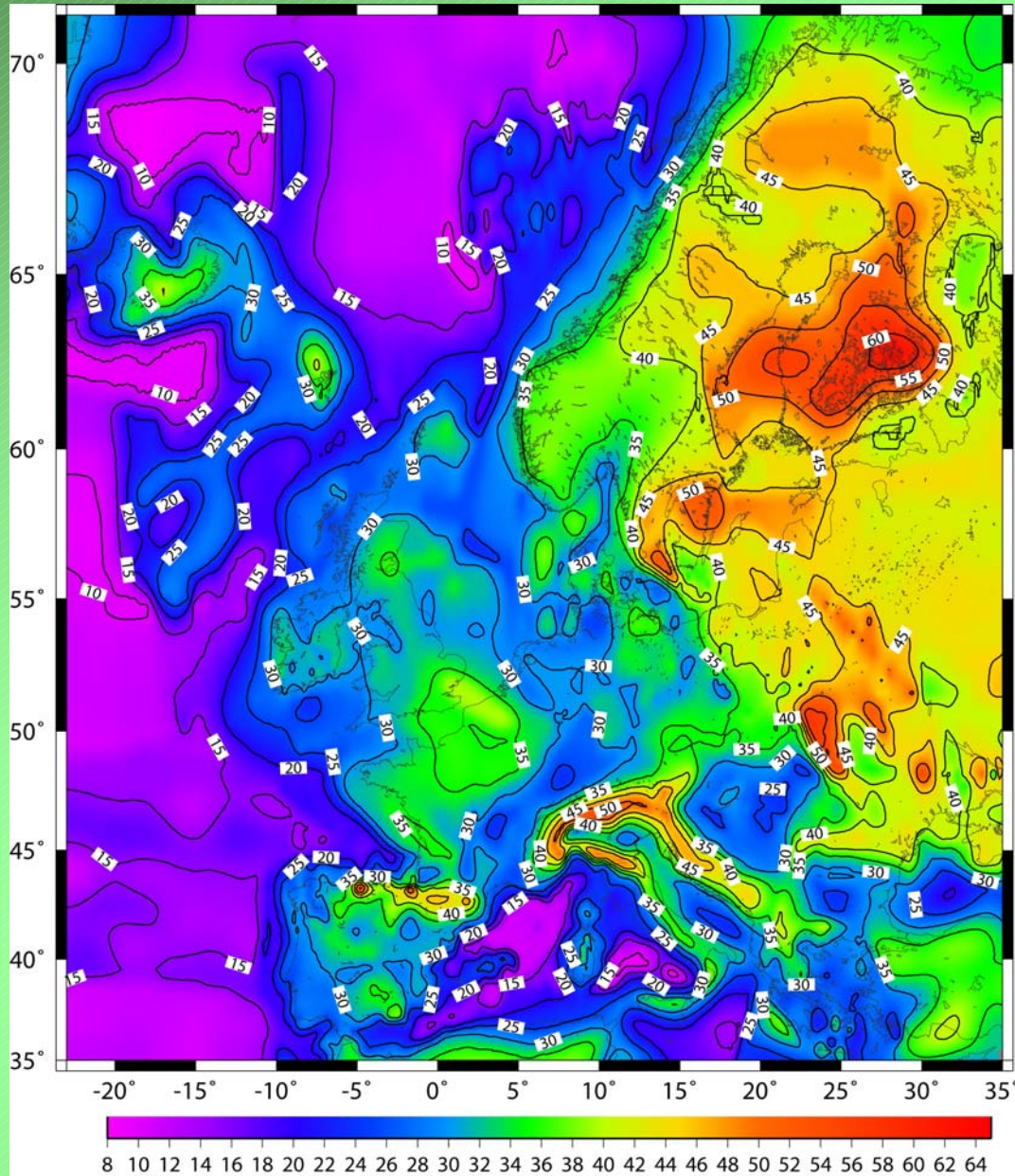




# Moho Map



# Moho Map

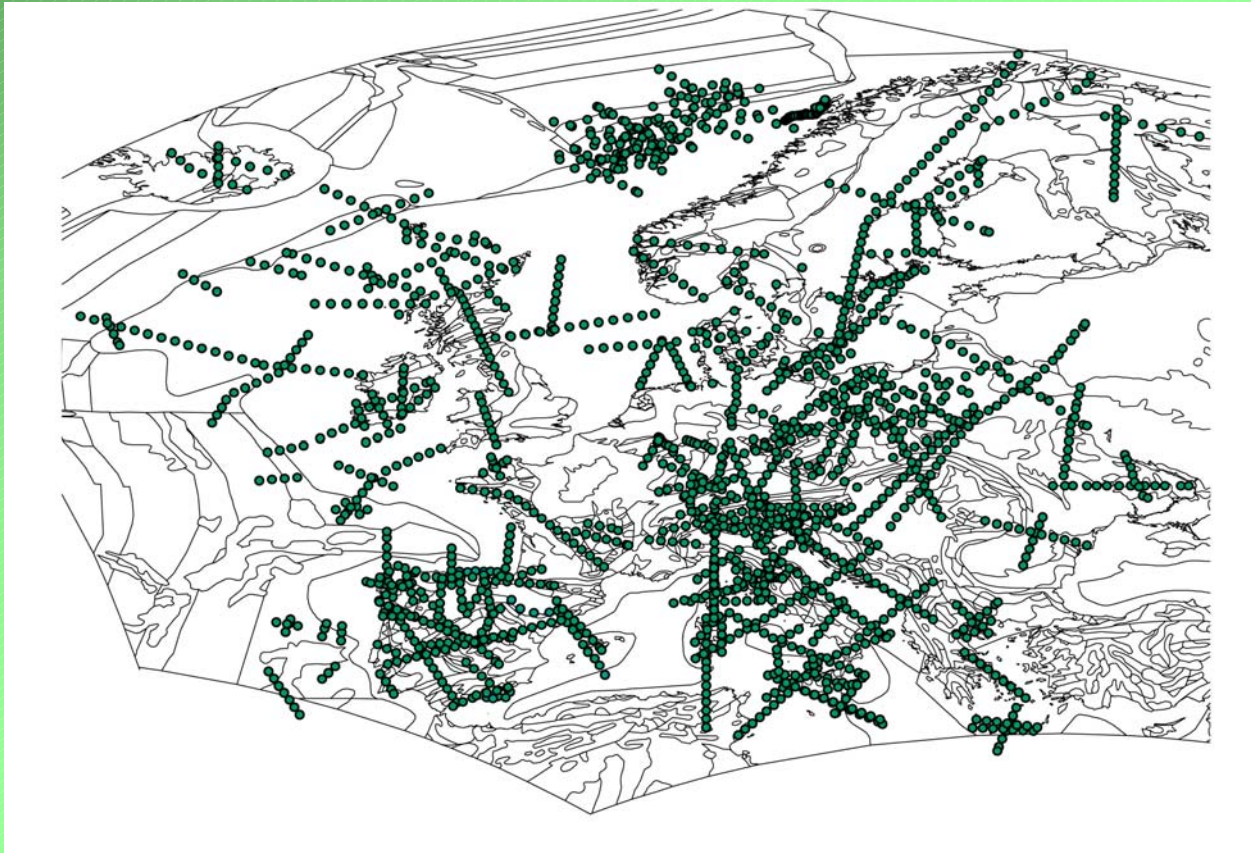




- Other crystalline crust discontinuities
- P-Wave average velocity within the layers

↓  
**Seismic profiles**

(e.g. CELEBRATION 2000, EGT, EUGENOS)



- Interpolation of seismic data where the coverage is good
- Seismic profile representative of geological feature

## Application of the crustal model:

- Seismic tomography
- Determination the lithology and the density of the European crust and upper mantle
- More accurate strength prediction
- Calculation of the contribution of the crust to the observed gravity field





# A new crustal model as input for the European strength map

M. Tesauro,<sup>(1,2)</sup> M. Kaban,<sup>(2)</sup> S. Cloetingh<sup>(1)</sup>

- (1) Netherlands Research Centre for Integrated Solid Earth science, Faculty of Earth and Life Science, Vrije Universiteit
- (2) GeoForschungsZentrum Potsdam (GFZ)



**Abstract**  
Tectonic studies made in intraplate Europe (Fig.1) have shown that this area is more active than would be expected from its location far away from plate boundaries. Intraplate Europe is characterized by horizontal and vertical motions with deformation rates of the order of 1-2 mm/yr and by diffuse seismicity (Nocquet and Calais, 2003; Tesauro et al., 2005). The first strength map (Cloetingh et al., 2005) has led to a significant understanding of the dynamics of intra-lithospheric deformation processes. The results have demonstrated that the European lithosphere is characterized by large spatial mechanical strength variations, with a pronounced contrast between the strong lithosphere of the East-European Platform (EEP) east of the Tesevye-Tornquist Zone (TTZ) and the relatively weak lithosphere of Western Europe. In order to improve the previous results and to extend the strength calculations to the southern and western plate boundaries of Eurasia, we are going to construct a new crustal model, which is a part of a comprehensive lithosphere model. As a first result, we demonstrate the new Moho map of Europe (Fig. 3). The Moho depth variations are reconstructed by merging the most recent maps existing for the European regions (e.g. Ziegler and Dözes, 2002; Kozlovskaja et al., 2004) and compiled by ourselves (Fig. 2) using published interpretations of seismic profiles (e.g. in the Voring and Lofoten basins). Strong differences in the crustal structure are found between the areas east and west of the TTZ, respectively. The eastern region is mostly characterized by thick crust, e.g. over the Baltic region (~42 km) with a maximum of over 60 km in the Baltic Shield. By contrast, crustal structure is more heterogeneous to the west from TTZ, being characterized by Variscan crust with an average thickness of 30-35 km, orogens (e.g. the Alps and the Pyrenees), where the crustal thickness is increased up to 45-50 km, and locally by strong extensional deformation, which resulted in a very thin crust in the Pannonian Basin (~25 km) and in the Tyrrhenian Sea (~10 km). Concerning the oceanic domain, the crustal thickness is generally decreased towards the ridge (up to 10 km in the most western part), with local maxima up to 20-25 km (e.g. in the Voring and Lofoten basins) and up to 35-40 km beneath the islands (e.g. Iceland and Faeroe islands), on account of mantle underplating. We calculated gravity effect of the Moho variations (Fig. 3) and density variations within the crust (Kaban, 2001) and removed it from the observed gravity field, which gives the residual mantle anomalies (Fig. 4). Since the upper mantle density is supposed to be constant in the reference model (3.35 g/cm<sup>3</sup>), the residual anomalies chiefly reflect the effect of mantle density variations (Kaban, 2001; 2002; Kaban, 2004). The mantle anomalies are clearly separated into two components possibly accounting for the effects of different factors:

- (1) A long-wavelength component reflects large-scale structural heterogeneities of the Eurasia lithosphere, supposedly related to its thermal regime in the study area. The TTZ divides EEP, which is characterized by predominantly positive anomalies from Western Europe with mostly negative mantle anomalies.
- (2) A regional relatively short-wavelength component (L < 2000 km) (Fig. 3) correlates with specific tectonic structures. A chain of negative mantle anomalies (-1-100 mGal) is found west of the TTZ (Pannonian basin, Rhine Graben and Massif Central). A very distinctive positive anomaly (>100 mGal) is located over the Carpathians and the Adriatic Sea, supporting the idea about strong lithospheric blocks.

**References**  
Cloetingh, S., Dierckx, P.A., Beaudin, F., Andriessen, P.M., Kaban, M., Kaban, G., Cloetingh, S., 2005. Lithospheric strength maps of stress and deformation variations across the Eurasian lithosphere. *Journal of Geophysical Research*, 110, F03106.  
Kaban, M., 2001. A Gravity Model of the North Eurasian Crust and Upper Mantle. *Journal of Geophysical Research*, 106, 13497-13510.  
Kaban, M., 2002. A Gravity Model of the North Eurasian Crust and Upper Mantle. *Journal of Geophysical Research*, 107, 4105-4118.  
Kaban, M., 2004. A Gravity Model of the North Eurasian Crust and Upper Mantle. *Journal of Geophysical Research*, 109, 4105-4118.  
Kaban, M., 2005. A Gravity Model of the North Eurasian Crust and Upper Mantle. *Journal of Geophysical Research*, 110, 4105-4118.  
Kaban, M., 2006. A Gravity Model of the North Eurasian Crust and Upper Mantle. *Journal of Geophysical Research*, 111, 4105-4118.  
Kaban, M., 2007. A Gravity Model of the North Eurasian Crust and Upper Mantle. *Journal of Geophysical Research*, 112, 4105-4118.  
Kaban, M., 2008. A Gravity Model of the North Eurasian Crust and Upper Mantle. *Journal of Geophysical Research*, 113, 4105-4118.  
Kaban, M., 2009. A Gravity Model of the North Eurasian Crust and Upper Mantle. *Journal of Geophysical Research*, 114, 4105-4118.  
Kaban, M., 2010. A Gravity Model of the North Eurasian Crust and Upper Mantle. *Journal of Geophysical Research*, 115, 4105-4118.  
Kaban, M., 2011. A Gravity Model of the North Eurasian Crust and Upper Mantle. *Journal of Geophysical Research*, 116, 4105-4118.  
Kaban, M., 2012. A Gravity Model of the North Eurasian Crust and Upper Mantle. *Journal of Geophysical Research*, 117, 4105-4118.  
Kaban, M., 2013. A Gravity Model of the North Eurasian Crust and Upper Mantle. *Journal of Geophysical Research*, 118, 4105-4118.  
Kaban, M., 2014. A Gravity Model of the North Eurasian Crust and Upper Mantle. *Journal of Geophysical Research*, 119, 4105-4118.  
Kaban, M., 2015. A Gravity Model of the North Eurasian Crust and Upper Mantle. *Journal of Geophysical Research*, 120, 4105-4118.  
Kaban, M., 2016. A Gravity Model of the North Eurasian Crust and Upper Mantle. *Journal of Geophysical Research*, 121, 4105-4118.  
Kaban, M., 2017. A Gravity Model of the North Eurasian Crust and Upper Mantle. *Journal of Geophysical Research*, 122, 4105-4118.  
Kaban, M., 2018. A Gravity Model of the North Eurasian Crust and Upper Mantle. *Journal of Geophysical Research*, 123, 4105-4118.  
Kaban, M., 2019. A Gravity Model of the North Eurasian Crust and Upper Mantle. *Journal of Geophysical Research*, 124, 4105-4118.  
Kaban, M., 2020. A Gravity Model of the North Eurasian Crust and Upper Mantle. *Journal of Geophysical Research*, 125, 4105-4118.  
Kaban, M., 2021. A Gravity Model of the North Eurasian Crust and Upper Mantle. *Journal of Geophysical Research*, 126, 4105-4118.  
Kaban, M., 2022. A Gravity Model of the North Eurasian Crust and Upper Mantle. *Journal of Geophysical Research*, 127, 4105-4118.  
Kaban, M., 2023. A Gravity Model of the North Eurasian Crust and Upper Mantle. *Journal of Geophysical Research*, 128, 4105-4118.  
Kaban, M., 2024. A Gravity Model of the North Eurasian Crust and Upper Mantle. *Journal of Geophysical Research*, 129, 4105-4118.  
Kaban, M., 2025. A Gravity Model of the North Eurasian Crust and Upper Mantle. *Journal of Geophysical Research*, 130, 4105-4118.

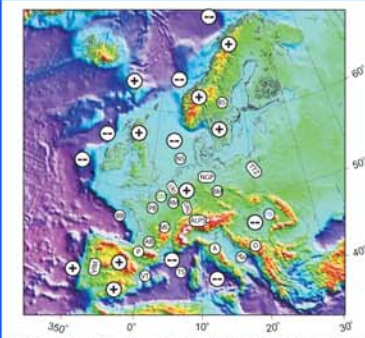


**Fig. 1** Topographic map of Europe. Intraplate areas of Late Neogene uplift and subsidence are displayed by circles with plus and minus symbols, respectively. Background elevation image is extracted from the ETOPO2 data set. The principal geological units of intraplate Europe are: East European Platform (EEP), Baltic Shield (BS), Tesevye-Tornquist zone (TTZ), Carpathians (C), Pannonian Basin (PB), North German Plain (NGP), Bohemian Massif (BM), Dinardic (D), North Sea (NS), Lower Rhine Graben (LRG), Upper Rhine Graben (URG), Rhinisch Massif (RM), Brabant Massif (BM), Paris Basin (PB), Massif Central (MC), Bay of Biscay (BB), Aquitaine Basin (AB), Pyrenees (P), Variscan Iberian Platform (VIM), Valencia Trough (VT), Tyrrhenian Sea (TS), Gibraltar Arc (GA), Adriatic Plate (AP), Apennines (A), Ionian Sea (IS).

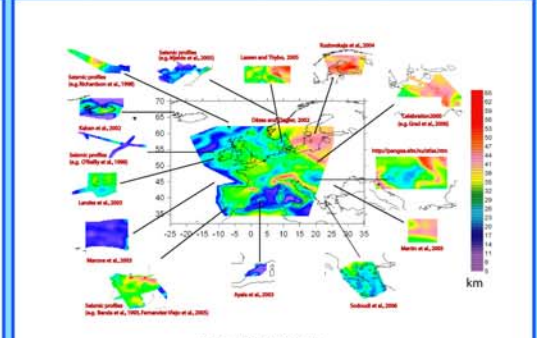


**Fig. 2** Compilations of Moho depth maps from various studies across Europe, showing different interpretations and depth scales.

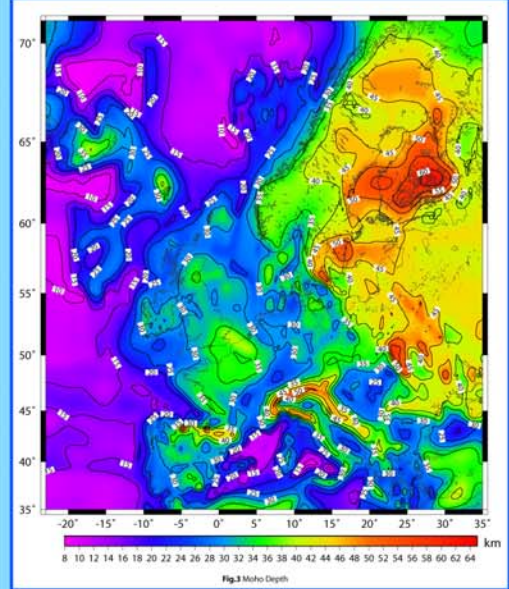


**Fig. 3** Moho Depth map of Europe showing depth variations in km.

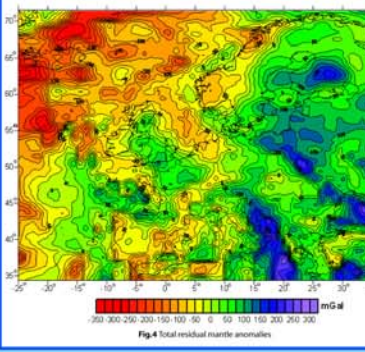


**Fig. 4** Total residual mantle anomalies map showing density variations in mg/d.

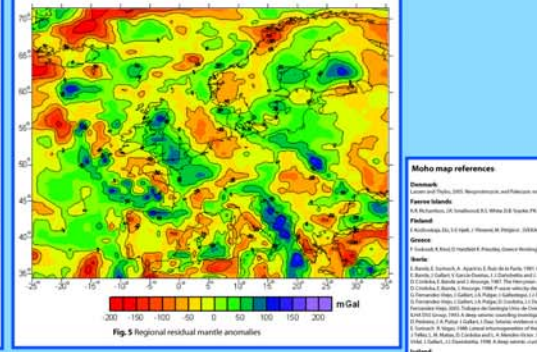


**Fig. 5** Regional residual mantle anomalies map showing density variations in mGal.

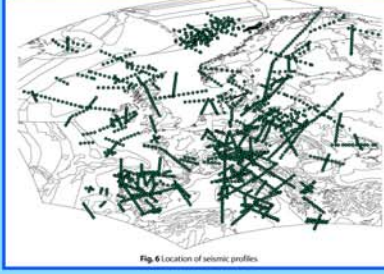


**Fig. 6** Location of seismic profiles across Europe.

**Moho map references**

Lorenzoni, S., 2005. Interpretation and discussion of Moho topography. *Geophysical Research Letters*, 32, L16306.  
Ferreira, M., 2001. Moho topography of the Iberian Peninsula and the surrounding regions. *Journal of Geophysical Research*, 106, 13497-13510.  
Ferreira, M., 2002. Moho topography of the Iberian Peninsula and the surrounding regions. *Journal of Geophysical Research*, 107, 4105-4118.  
Ferreira, M., 2003. Moho topography of the Iberian Peninsula and the surrounding regions. *Journal of Geophysical Research*, 108, 4105-4118.  
Ferreira, M., 2004. Moho topography of the Iberian Peninsula and the surrounding regions. *Journal of Geophysical Research*, 109, 4105-4118.  
Ferreira, M., 2005. Moho topography of the Iberian Peninsula and the surrounding regions. *Journal of Geophysical Research*, 110, 4105-4118.  
Ferreira, M., 2006. Moho topography of the Iberian Peninsula and the surrounding regions. *Journal of Geophysical Research*, 111, 4105-4118.  
Ferreira, M., 2007. Moho topography of the Iberian Peninsula and the surrounding regions. *Journal of Geophysical Research*, 112, 4105-4118.  
Ferreira, M., 2008. Moho topography of the Iberian Peninsula and the surrounding regions. *Journal of Geophysical Research*, 113, 4105-4118.  
Ferreira, M., 2009. Moho topography of the Iberian Peninsula and the surrounding regions. *Journal of Geophysical Research*, 114, 4105-4118.  
Ferreira, M., 2010. Moho topography of the Iberian Peninsula and the surrounding regions. *Journal of Geophysical Research*, 115, 4105-4118.  
Ferreira, M., 2011. Moho topography of the Iberian Peninsula and the surrounding regions. *Journal of Geophysical Research*, 116, 4105-4118.  
Ferreira, M., 2012. Moho topography of the Iberian Peninsula and the surrounding regions. *Journal of Geophysical Research*, 117, 4105-4118.  
Ferreira, M., 2013. Moho topography of the Iberian Peninsula and the surrounding regions. *Journal of Geophysical Research*, 118, 4105-4118.  
Ferreira, M., 2014. Moho topography of the Iberian Peninsula and the surrounding regions. *Journal of Geophysical Research*, 119, 4105-4118.  
Ferreira, M., 2015. Moho topography of the Iberian Peninsula and the surrounding regions. *Journal of Geophysical Research*, 120, 4105-4118.  
Ferreira, M., 2016. Moho topography of the Iberian Peninsula and the surrounding regions. *Journal of Geophysical Research*, 121, 4105-4118.  
Ferreira, M., 2017. Moho topography of the Iberian Peninsula and the surrounding regions. *Journal of Geophysical Research*, 122, 4105-4118.  
Ferreira, M., 2018. Moho topography of the Iberian Peninsula and the surrounding regions. *Journal of Geophysical Research*, 123, 4105-4118.  
Ferreira, M., 2019. Moho topography of the Iberian Peninsula and the surrounding regions. *Journal of Geophysical Research*, 124, 4105-4118.  
Ferreira, M., 2020. Moho topography of the Iberian Peninsula and the surrounding regions. *Journal of Geophysical Research*, 125, 4105-4118.  
Ferreira, M., 2021. Moho topography of the Iberian Peninsula and the surrounding regions. *Journal of Geophysical Research*, 126, 4105-4118.  
Ferreira, M., 2022. Moho topography of the Iberian Peninsula and the surrounding regions. *Journal of Geophysical Research*, 127, 4105-4118.  
Ferreira, M., 2023. Moho topography of the Iberian Peninsula and the surrounding regions. *Journal of Geophysical Research*, 128, 4105-4118.  
Ferreira, M., 2024. Moho topography of the Iberian Peninsula and the surrounding regions. *Journal of Geophysical Research*, 129, 4105-4118.  
Ferreira, M., 2025. Moho topography of the Iberian Peninsula and the surrounding regions. *Journal of Geophysical Research*, 130, 4105-4118.

**Voring and Lofoten basins**

Beck, M., 2001. Moho topography of the Voring and Lofoten basins. *Journal of Geophysical Research*, 106, 13497-13510.  
Beck, M., 2002. Moho topography of the Voring and Lofoten basins. *Journal of Geophysical Research*, 107, 4105-4118.  
Beck, M., 2003. Moho topography of the Voring and Lofoten basins. *Journal of Geophysical Research*, 108, 4105-4118.  
Beck, M., 2004. Moho topography of the Voring and Lofoten basins. *Journal of Geophysical Research*, 109, 4105-4118.  
Beck, M., 2005. Moho topography of the Voring and Lofoten basins. *Journal of Geophysical Research*, 110, 4105-4118.  
Beck, M., 2006. Moho topography of the Voring and Lofoten basins. *Journal of Geophysical Research*, 111, 4105-4118.  
Beck, M., 2007. Moho topography of the Voring and Lofoten basins. *Journal of Geophysical Research*, 112, 4105-4118.  
Beck, M., 2008. Moho topography of the Voring and Lofoten basins. *Journal of Geophysical Research*, 113, 4105-4118.  
Beck, M., 2009. Moho topography of the Voring and Lofoten basins. *Journal of Geophysical Research*, 114, 4105-4118.  
Beck, M., 2010. Moho topography of the Voring and Lofoten basins. *Journal of Geophysical Research*, 115, 4105-4118.  
Beck, M., 2011. Moho topography of the Voring and Lofoten basins. *Journal of Geophysical Research*, 116, 4105-4118.  
Beck, M., 2012. Moho topography of the Voring and Lofoten basins. *Journal of Geophysical Research*, 117, 4105-4118.  
Beck, M., 2013. Moho topography of the Voring and Lofoten basins. *Journal of Geophysical Research*, 118, 4105-4118.  
Beck, M., 2014. Moho topography of the Voring and Lofoten basins. *Journal of Geophysical Research*, 119, 4105-4118.  
Beck, M., 2015. Moho topography of the Voring and Lofoten basins. *Journal of Geophysical Research*, 120, 4105-4118.  
Beck, M., 2016. Moho topography of the Voring and Lofoten basins. *Journal of Geophysical Research*, 121, 4105-4118.  
Beck, M., 2017. Moho topography of the Voring and Lofoten basins. *Journal of Geophysical Research*, 122, 4105-4118.  
Beck, M., 2018. Moho topography of the Voring and Lofoten basins. *Journal of Geophysical Research*, 123, 4105-4118.  
Beck, M., 2019. Moho topography of the Voring and Lofoten basins. *Journal of Geophysical Research*, 124, 4105-4118.  
Beck, M., 2020. Moho topography of the Voring and Lofoten basins. *Journal of Geophysical Research*, 125, 4105-4118.  
Beck, M., 2021. Moho topography of the Voring and Lofoten basins. *Journal of Geophysical Research*, 126, 4105-4118.  
Beck, M., 2022. Moho topography of the Voring and Lofoten basins. *Journal of Geophysical Research*, 127, 4105-4118.  
Beck, M., 2023. Moho topography of the Voring and Lofoten basins. *Journal of Geophysical Research*, 128, 4105-4118.  
Beck, M., 2024. Moho topography of the Voring and Lofoten basins. *Journal of Geophysical Research*, 129, 4105-4118.  
Beck, M., 2025. Moho topography of the Voring and Lofoten basins. *Journal of Geophysical Research*, 130, 4105-4118.

**Future perspectives**

The results of deep seismic reflection and refraction and/or receiver function studies (Fig. 6) will be used to define the depth of the crustal interfaces and P-wave velocity distribution in order to complete the new crustal model. Furthermore, in the next stage, seismic tomography data will be used to get the location of the lithosphere-atmosphere boundary and calculate the temperature distribution. These results, jointly with the new crustal model, will allow us to recalculate a strength state of the European lithosphere and to construct a new density model.